Harmaline Attenuates Voltage - Sensitive Ca^{2+} Currents in Neurons of the Inferior Olive

Xiping Zhan [1,2,*], Werner M Graf [2]

[1] Department of Neuroscience, Johns Hopkins University School of Medicine,
[2] Department of Physiology and Biophysics, Howard University College of Medicine

Received, October 18, 2012; Revised, November 16, 2012; Accepted, December 7, 2012; Published, December 11, 2012.

ABSTRACT - Purpose. Harmaline is one member of a class of tremorgenic harmala alkaloids that have been implicated in neuroprotective effects and neurodegenerative disorders. It has been reported to interact with several neurotransmitter receptors as well as ion exchangers and voltage-sensitive channels. One site of harmaline action in the brain is the inferior olive (IO). Either local or systemic harmaline injection has been reported to increase spiking rate and coherence in the inferior olive and this activation is thought to produce tremor and ataxia through inferior olivary neuron activation of target neurons in the cerebellum, but the cellular mechanism is not yet known. **Methods.** Here, we have performed whole cell voltage-clamp and current clamp recordings from olivary neurons in brain slices derived from newborn rats. **Results.** We found that both transient low-voltage activated (LVA) and sustained high voltage-activated (HVA) Ca^{2+} currents are significantly attenuated by 0.125 – 0.25 mM harmaline applied to the bath and that this attenuation is partially reversible. In current clamp recordings, spike-afterhyperpolarization complexes were evoked by brief positive current injections. Harmaline produced a small attenuation of spike amplitude, but large spike broadening associated with attenuation of the fast and medium afterhyperpolarization. **Conclusion.** Our data suggest that one mode of olivary neuron activation by harmaline involves attenuation of both HVA and LVA Ca^{2+} conductances and consequent attenuation of Ca^{2+}-sensitive K^+ conductances resulting in spike broadening and attenuation of the afterhyperpolarization. Both of HVA and LVA attenuation also suggests a role to regulate intracelluar Ca^{2+}, thereby to protect neurons from apoptosis.

INTRODUCTION

Harmaline is a β-carboline, which, together with related compounds harmane and norharmane, is present in the human food chain. These compounds have been detected in a wide variety of tissues including liver, heart, kidney, blood and brain. Their pharmacolgical actions are broad: they have been reported to bind GABA-A receptors (1, 2), activate $5HT_2A$ and $5HT_2C$ receptors (3), block Na^+-proton exchange (4, 5), and protect apoptosis by inhibiting monoamine oxidase (6).

A prominent toxic effect of harmaline is that its use produces a stereotyped generalized tremor in a number of mammalian species (7-10) and has been proposed as a model for essential tremor seen in certain neurodegenerative diseases (11-14). Both recording and lesion studies have indicated that the main target for harmaline in inducing tremor is the inferior olive (IO) (9, 15-17). Recordings have shown that harmaline activation of the inferior olive results in enhanced activity which is transmitted to the cerebellar cortex by climbing fibers. Transection of the inferior cerebellar peduncle, where the climbing fibers run, blocks harmaline-induced tremor (16), indicating that cerebellar activation is required.

How does harmaline activate the neurons of the inferior olive? Classic microelectrode current clamp recordings by Llinás and Yarom (1986) first characterized two modes of action of harmaline in inferior olivary neurons: hyperpolarization, resulting in deinactivation of LVA Ca^{2+} channels, and a positive shift of the activation curve for low threshold Ca^{2+} spikes (18). More recently, LVA current was suggested to be carried by T-type channel $Ca_v3.1$ that plays an essential role (17).

Corresponding Author: Xiping Zhan, 520 W Street, Washington, DC; Email: xipingzhan@yahoo.com

This notion is further substantiated by the fact that hamaline induced tremor can be suppressed by T-type antagonists (19). In the inferior olive, HVA, mostly carried by the P/Q channel $Ca_v2.1$ subunit (20) is closely regulated with LVA and is also implicated in IO rhythmicity (21). The disturbance of IO rhythmicity underlies the etiology of essential tremor. However, it is still elusive how LVA interacts with other conductances such as HVA and Ca^{2+} dependant potassium currents under harmaline efffects.

In addition to its toxic effect on Purkinje cells (45) caused by increased olivary neuronal excitability, harmaline is also implicated to have a neuroprotective effect against neuronal apoptosis (22), as it attenuates Ca^{2+} entry to reduce intracellular Ca^{2+}, a critical process for Ca^{2+} apoptosis (23). The LVA current is transient, and HVA is sustained. The relevant conductances are distributed differentially on somata and distal dendrites, implicating different roles in Ca^{2+} homeostasis. Additionally, HVA is suggested to be more sensitive to harmaline than LVA (22). Here we have revisited these issues and examined both HVA and LVA channels by recording from olivary neurons in brain slices of newborn rats using whole-cell patch clamp recording techniques that allow for voltage-clamp and current-clamp analysis. Part of this paper was reported as an abstract at 2012 Neuroscience Meeting, New Orleans.

MATERIALS AND METHODS

Preparation of slices containing the inferior olive

Sprague-Dawley rats, 11 to 14 days old (either sex, Charles River), were anesthetized with isoflurane and decapitated with a guillotine. The bone and dura covering the cortical surface were carefully peeled away and the brain was removed. The rostral part of the brain was glued to the stage of a Leica VT1000S vibrating slicer and submerged in a chamber containing ACSF in which Na^+ was substituted with glycerol (in mM: glycerol, 208; NaHCO3, 26; NaH_2PO4 1.25; KCl, 5; MgSO4, 3; $CaCl_2$, 0.5; Na-L-ascorbate; 10; Na-pyruvate, 3; glucose, 10) (24). This solution was aerated with 95% O_2 and 5% CO_2 yielding a pH of 7.4. Five or six transverse slices (250–300 μm thick) were obtained by slicing the region between the spinal cord and the rostral part of the cerebellar cortex. The slices were allowed to recover in an incubation chamber at 35°C for at least 30 min. The chamber contained normal artificial cerebrospinal fluid solution (in mM: NaCl, 124; KCl, 2.5; $MgCl_2$, 1.3; $CaCl_2$ 2.5; NaH_2PO4, 1; $NaHCO_3$, 26.2; glucose, 20; pH 7.4, equilibrated with 95% O_2 and 5% CO_2, ~310 mosm). Animal use and experimental methods were approved by the Institutional Animal Care and Use Committee of the Johns Hopkins University School of Medicine.

Whole-Cell Recordings

Voltage-clamp recordings were made at 30-33°C in a chamber perfused with modified ACSF (in mM: NaCl, 112; KCl, 2.5; $MgCl_2$, 1; $CaCl_2$ 2.5; NaH_2PO_4, 1; $NaHCO_3$, 26; glucose, 22 ; tetraethylammonium-Cl, 10; tetrodotoxin, 0.0005; pH 7.4) which flowed at 4 ml/min. Patch electrodes were pulled from borosilicate glass and had resistances of 1.5 - 2.0 MΩ when filled with a Cs-based intracellular solution for voltage clamp recording (in mM: CsF, 103; NaCl, 5; Hepes, 10; EGTA free acid, 10; Na_2-ATP, 4; GTP, 0.4; $MgCl_2$, 4; $CaCl_2$, 1; QX-314-Br, 1; tetraethylamonium-Cl, 10; phosphocreatine-tris, 7; pH 7.3, ~290 mosm).

The inferior olive was identified in the slices using a 5x objective mounted on an upright microscope with transmitted light, and the olivary neuron somata were then visualized through a 40x water immersion objective using infrared differential interference contrast optics (Figure S1). Whole-cell somatic recordings were made using an Axopatch 200B amplifier in combination with PCLAMP 9.0 software (Molecular Devices). Cells were voltage–clamped at –80 mV. R_{series} and R_{input} were monitored using a 2.5 mV 100 ms depolarizing voltage step in each recording sweep, and recordings were discontinued if changes in R_{series} or R_{input} were larger than 20%, or if changes in baseline current amplitudes were larger than 10%. Current traces were filtered at 1 kHz, and digitized at 10 kHz using a Digidata 1322A interface, and stored for off-line analysis. Ca^{2+} currents were corrected for leak and capacitative currents by subtracting a scaled current elicited by a +5 mV step from the holding potential.

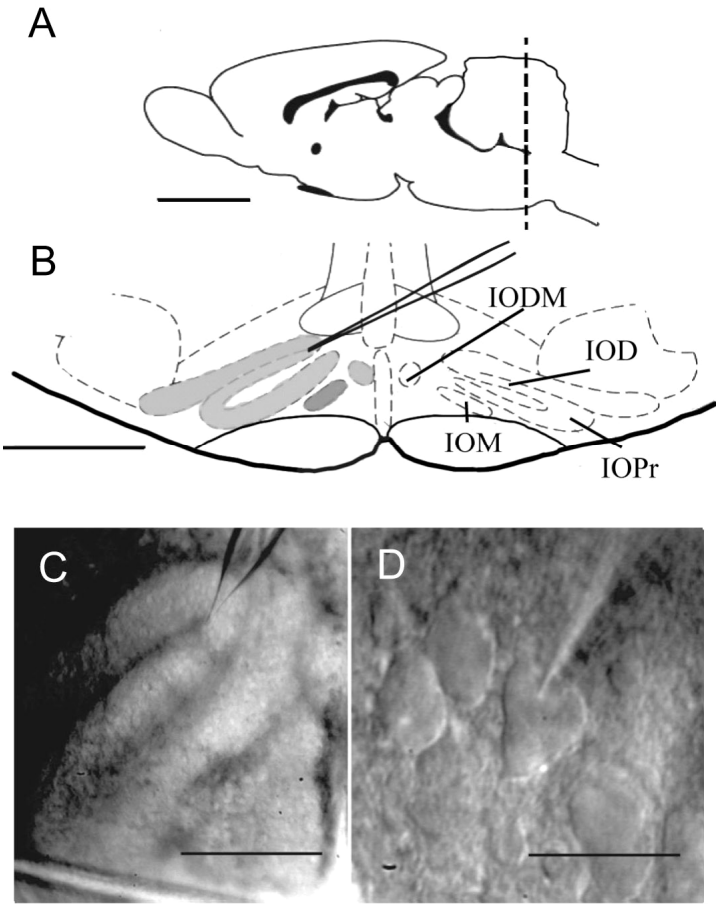

Figure S1. An illustration of the recording location in the inferior olive. A) The plane of a coronal section for a brain slice. B) The location of recording illustrated in an adult rat brain atlas. The inferior olive is shaded on the left side. IOM, inferior olive nucleus, medial; IOD, inferior olive nucleus, dorsal; IODM, inferior olive nucleus, dorsal medial subnucleus; IOPr, principle inferior olive nucleus, rostral subnucleus. C) Low power transmitted light view of the inferior olive. D) High power view of olivary neuron soma with patch pipette using DIC optics. Scale bars: A, 5 mm; B, 1 mm; C, 0.5 mm; D, 20 μm.

For current clamp recording, the same external saline was used and the internal saline contained (in mM): K-Gluconate,122; NaCl, 9; $MgCl_2$,1.8; Na_2-ATP, 4; GTP, 0.4; Hepes, 9; EGTA, 0.5; phosphocreatine-tris; 14 (pH 7.3, 290 mosm). Using an Axopatch 200B amplifier, whole cell mode was achieved initially in the voltage clamp configuration. Then, the recording was switched into current clamp mode. The resting membrane potential was monitored for more than ten minutes. The experiment was discontinued if the resting membrane potential became more positive than -40 mV. The action potential traces were filtered at 5 kHz, and digitized at 10 kHz. The action potential was continually monitored for six minutes, and if there was no threshold change, the harmaline perfusion commenced. All group data are reported as mean ± SEM. All *P* values were determined against controls, using a two-tailed Student's t-test to determine significance between the groups; $P<0.05$ was considered statistically significant.

RESULTS

The recordings described in this paper were obtained from 86 neurons in the principal and medial accessory olivary subnuclei (25). Whole cell recordings from visualized olivary neuron somata were performed (Figure S1). In order to isolate voltage-sensitive Ca^{2+} currents, recordings were made using a Cs/TEA-based internal saline supplemented with QX-314 and a Na^+-based external saline supplemented with TTX and TEA. Low QX-134 was used to block sodium channels

without significantly affecting both LVA and HVA Ca^{2+} currents (26, 27). In contrast to Park et al (17), we either did not use HVA blocker in the intracellular solution or in the external ACSF so that we could examine both HVA and LVA simultaneously. To record voltage-sensitive Ca^{2+} currents, the command voltage was initially set to -80 mV and 100 msec long depolarizing steps were then delivered to a series of target voltages to evoke Ca^{2+} currents (Figure 1). In some cases, the depolarizing pulse was preceded by a 50 msec long step hyperpolarization to -105 mV to deinactivate the channels of interest. Consistent with previous observations in other types of neurons, transient Ca^{2+} currents were elicited with low threshold steps (to about -55 mV) while sustained currents required larger depolarization (to about -30 mV). Also consistent with previous observations, the transient LVA Ca^{2+} currents were significantly potentiated by a hyperpolarizing prepulse while the sustained HVA currents were largely unaffected. For steps to -55 mV, without hyperpolarizing prepulses, the peak current amplitude was -1160 ± 226 pA (mean ± SEM, n = 9) and the sustained Ca^{2+} current, measured at the depolarizing pulse offset, was -63 ± 6 pA (Figure 1A). For steps to -30 mV, without hyperpolarizing prepulses, the peak current amplitude was -2640 ± 471 pA and the sustained Ca^{2+} current, measured at the depolarizing pulse offset, was -1787 ± 377 pA (Figure 1B). When hyperpolarizing prepulses were employed, for steps to -55 mV, the peak current amplitude was -1822 ± 286 pA (n = 9) and the sustained Ca^{2+} current, measured at the depolarizing pulse offset, was -70 ± 5 pA. For steps to -30 mV the peak current amplitude was -2916 ± 524 pA and the sustained Ca^{2+} current, measured at the depolarizing pulse offset, was 1813 ± 376 pA. Current-voltage relations showing the voltage dependence of activation are shown for an exemplar cell (left) and the entire population (right) in Figure 1B. These reveal that the deinactivation from the hyperpolarizing prepulse shifted the voltage dependence of LVA Ca^{2+} channel activation in the hyperpolarizing (leftward) direction.

Rundown is always a concern in sustained recording of voltage-sensitive currents (28-31). Figure 2 showed long-term control recordings to illustrate that rundown was minimal in our conditions. For steps to -55 mV, used to record transient LVA Ca^{2+} current in isolation, peak Ca^{2+} current at t = 35 min was 100 ± 3 % of baseline values (n= 6). For steps to -30 mV, used to record mixed transient and sustained HVA Ca^{2+} currents, peak Ca^{2+} current at t = 25 min was 100 ±3 % of baseline values, and sustained Ca^{2+} current at t = 25 min was 100 ± 5 % of baseline values (n=4). This recording condition is more stable than that (6 min) performed previously (22). Thus, the present conditions allowed for reasonably stable recordings of Ca^{2+} currents over the 25 min time course used here.

Following 8 min of baseline recording, harmaline (0.25 mM) was added to the bath, where it remained for 6 min before washout (Figure 3). Depolarizing steps to -55 mV evoked a transient LVA Ca^{2+} current, that was strongly attenuated by harmaline (60 ± 2 % of baseline at t = 15 min, n = 9; student test, $P<0.05$) and which showed partial recovery upon washout (84 ± 4 % of baseline at t = 30 min). When depolarizing steps to -30 mV were used, Ca^{2+} currents were evoked with both transient and sustained HVA components, both of which were attenuated (peak current: 75 ± 2 % of baseline; sustained current: 79 ± 2% of baseline, at t = 15 min, n = 7; student test, $P<0.01$) and both of which showed partial recovery upon washout (peak current: 88 ± 3 % of baseline at t = 25 min; sustained current: 84 ± 3 % of baseline at t = 25 min).

When this application protocol was repeated in different cells, now with a lower dose, 0.125 mM harmaline, attenuation of LVA was still observed ($P<0.05$, n=10; Dep= -55 mV; Figure 5), but the attenuation was not significant for HVA ($P>0.05$, n=8; Dep= -30 mV). LVA Ca^{2+} current, was strongly attenuated by harmaline (72 ± 2% of baseline at t = 15 min, n = 10), which showed partial recovery upon washout (81 ± 2% of baseline at t = 30 min). Both transient and sustained HVA components were attenuated (peak current: 82 ±2 % of baseline at t = 15 min; sustained current: 85 ± 2 % of baseline at t = 15 min, n = 8) and both showed partial recovery upon washout (peak current: 88 ± 2 % of baseline at t = 20 min; sustained current: 90 ± 2 % of baseline at t = 20 min). Similar results were seen when these experiments were performed without hyperpolarizing prepulses, which is closer to a normal physiological state (Figure 4 and 5). Figure 5 shows a bar graph summary of all of the experiments performed to evaluate the effects of harmaline on voltage-sensitive Ca^{2+} currents. The main finding: both LVA and HVA Ca^{2+} currents

were attenuated by 0.25 mM harmaline for the protocol with hyperpolarizing prepulses, although the effect of harmaline on LVA Ca^{2+} currents was sometimes not in parallel with that on HVA.

In a separate set of experiments, harmaline was applied to a cell recorded in current clamp mode with a K-based internal saline (Figure 6). The 23 olivary neurons recorded in current clamp mode showed a wide range of resting potentials, from -45 to -72 mV, with a mean of -53 ± 2 mV (mean ± sem). When harmaline (0.125 – 0.25 mM) was applied for 6 min, hyperpolarization was produced in 9 of 23 neurons (range: -7 to -33 mV; mean = -18± 2 mV) and no significant change was seen in the remaining 14 neurons (mean = +3 ± 1 mV). Interestingly, the hyperpolarization produced by bath-applied harmaline did not reverse, even upon sustained washout, in notable contrast to harmaline's effects on Ca^{2+} currents. Only 9 out of 23 olivary neurons recorded here showed subthreshold oscillations (data not shown), consistent with previous recordings in newborn tissues (32).

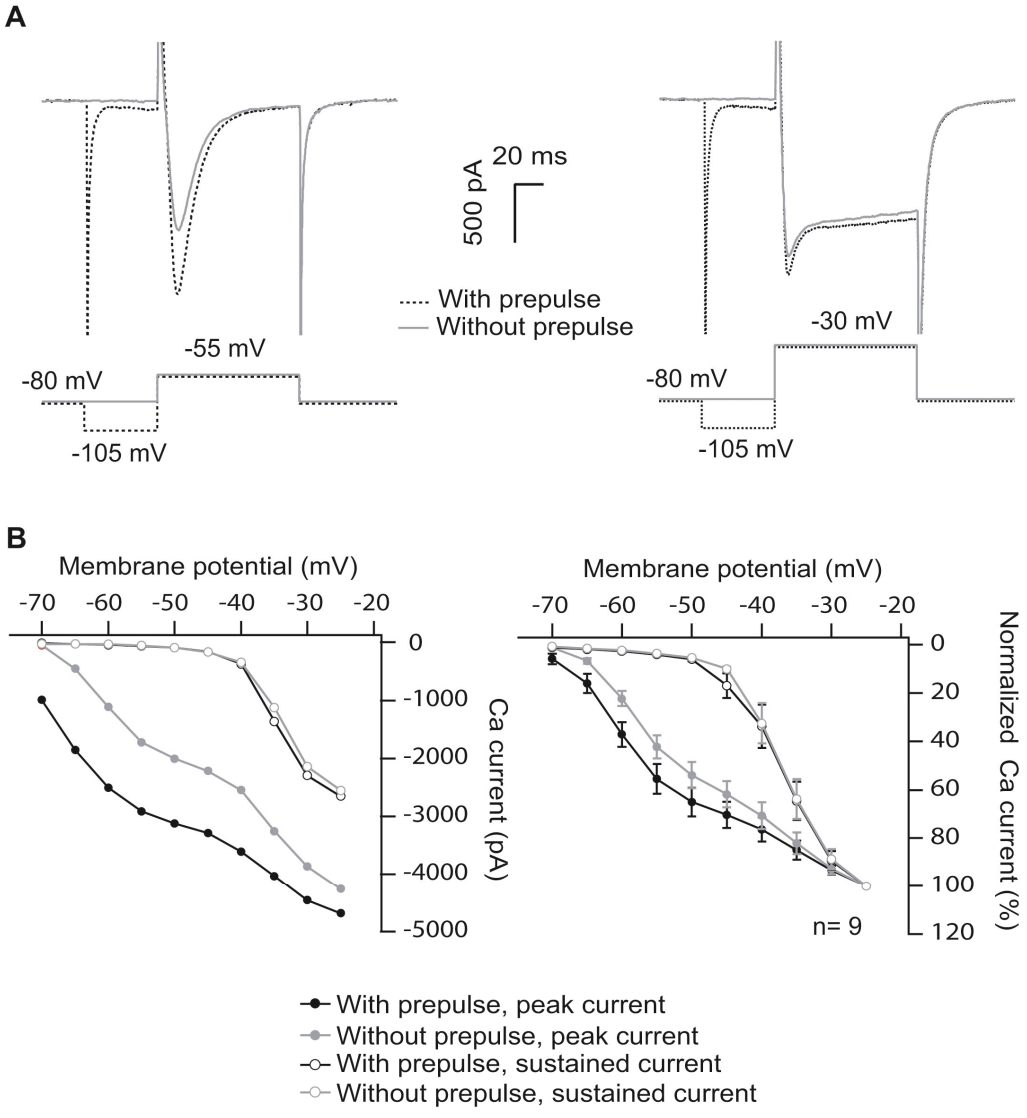

Figure 1. Voltage-sensitive Ca^{2+} currents recorded in olivary neurons. A) Representative current traces with and without a hyperpolarizing prepulse designed to deinactivate Ca^{2+} channels. B) Current voltage relations for a family of depolarizing current steps. The left panel shows a representative cell and the right panel shows the mean current amplitudes normalized to maximum current. Error bars represent SEM in this and all subsequent figures.

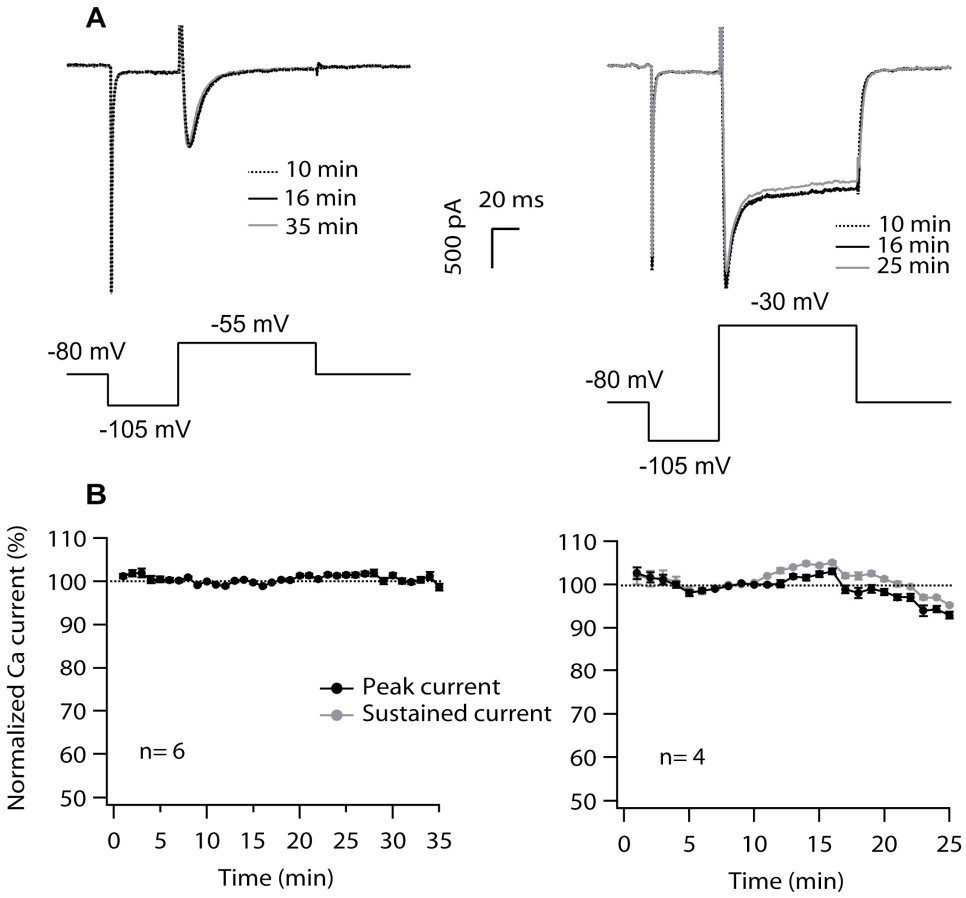

Figure 2. Voltage-sensitive Ca^{2+} currents can be recorded continuously in olivary neurons with minimal rundown. A) Exemplar current traces recorded from a single olivary neuron. Peak current is plotted for the LVA Ca^{2+} currents evoked by steps to -55 mV (left) while both peak and sustained Ca^{2+} current are plotted for HVA Ca^{2+} currents evoked by steps to -30 mV (right). B) Population time course records are normalized to the baseline period 6-8 min.

Action potentials were evoked by injection of depolarizing current (1.2 - 2.2 nA for 20 msec). As previously described (33, 34), current injection in neurons resting at more depolarized potentials, evoked spikes with a Ca^{2+} plateau around 0 mV (Figure 6A and C), while current injections in cells resting at more hyperpolarized potentials evoked spikes with a narrower Ca^{2+} plateau around -60 mV (Figure 6B). Harmaline produced a small attenuation of spike amplitude (90.8 ± 2.8 percent of baseline, n = 9). However, it should be cautioned that these recordings were made using an Axopatch 200B, which is not a true voltage-follower amplifier. Thus, fast events in current clamp, like the peak of the action potential, are subject to some distortion. In 8 of 19 neurons, harmaline produced a change characterized by a broadening of the spike and an attenuation of the afterhyperpolarization (AHP). An index of the spike width was determined by measuring the width duration at a point 15 mV depolarized from the resting potential. This was 20 ±2.7 msec before harmaline and 34 ± 4 msec after harmaline (n = 8). Exemplar traces showing this effect may be seen in Figure 6. Spike broadening in the subpopulation of cells hyperpolarized by harmaline showed an increase to 352 ± 68 percent of baseline (n= 2) and an increase to 133± 3 percent of baseline in those cells not hyperpolarized by harmaline (n = 6). In the 7 cells which showed a clear AHP, the AHP amplitude (measured as the peak amplitude difference from the resting potential) was reduced to 71 ± 10 % of baseline (n = 5) and the AHP latency (measured as the delay between the peak of the spike and the peak of the AHP was increased to 159.9 ± 17.1 percent of baseline. In another two cells, the AHP was slightly increased.

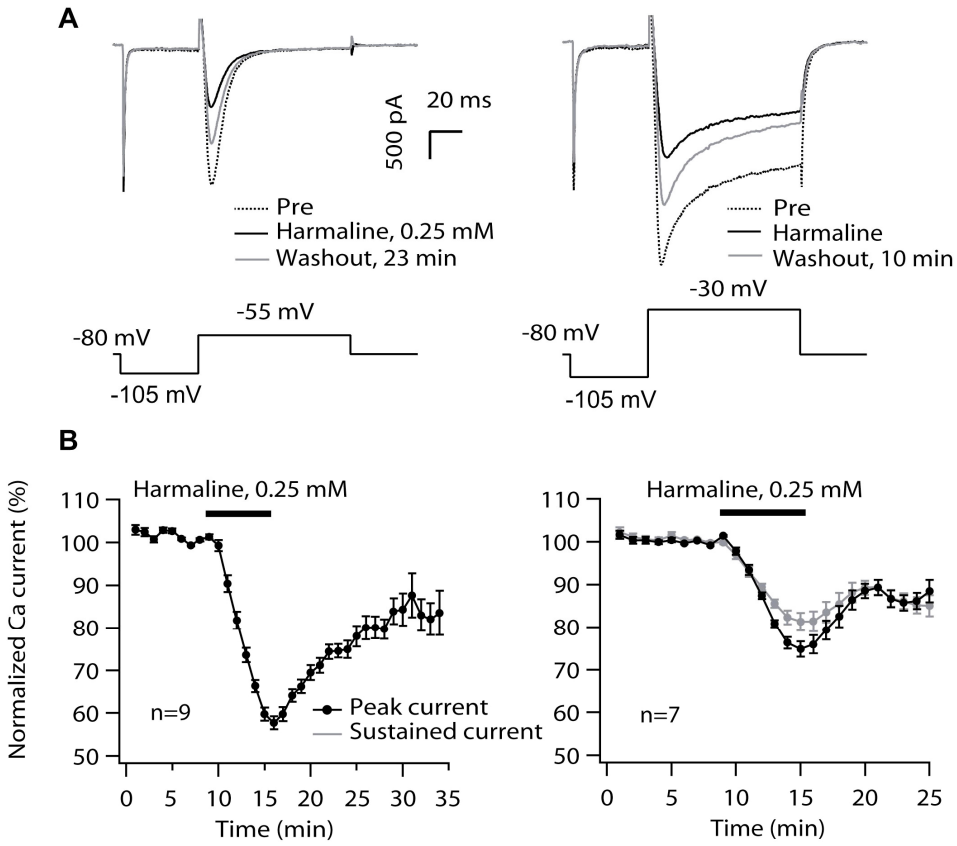

Figure 3. Harmaline, at a concentration of 0.25 mM, attenuates both LVA HVA Ca^{2+} currents. A) Exemplar current traces recorded from a single olivary neuron. Peak current is plotted for the LVA Ca^{2+} currents evoked by steps to -55 mV (left) while both peak and sustained Ca^{2+} current are plotted for HVA Ca^{2+} currents evoked by steps to -30 mV (right). B) Population time course records are normalized to the baseline period 6-8 min.

DISCUSSION

The main finding of this study is that harmaline, delivered at a concentration of 0.125 or 0.25 mM, attenuated both LVA and HVA Ca^{2+} currents in neurons of the inferior olive in brain slices derived from newborn rats. The concentrations we investigated for both voltage and current clamp recording are larger than that Park et al used (0.001~ 0.1 mM) for voltage clamp, but slightly smaller than that used for current clamp recording (0.1 mg/ml or 0.35 mM) (17). Thus, harmaline effects from voltage clamp and current clamp in our preparations are comparable. Albeit a smaller change, the HVA attenuation becomes apparent since we adopted a modified protocol that allows a longer harmaline perfusion to be monitored (Figure 2). A secondary finding is that, in current clamp recordings from these neurons, harmaline produced a significant alteration in evoked spikes, consisting of a broadening of the spike and attenuation of the AHP. This effect on spikes was sometimes, but not always, accompanied by hyperpolarization of the resting potential. One suggestion, which remains unproven, is the attenuation of Ca^{2+} currents produced by harmaline results in reduced activation of Ca^{2+}-sensitive K^+ conductances, thereby underlying its effects on the spike/AHP complex.

The present findings confirm some aspects of the microelectrode recordings of Llinás and Yarom (1986) in guinea pigs or Park et al in mice (17). Like them, we found that harmaline could sometimes produce a hyperpolarization of olivary neurons. They reported that the low-threshold Ca^{2+} spike (recorded in TTX) was activated at more positive potentials with harmaline, and suggested that harmaline shifts the voltage-dependence of deinactivation of LVA Ca^{2+} channels in the positive direction, thereby making more LVA Ca^{2+} channels available to open at positive potentials.

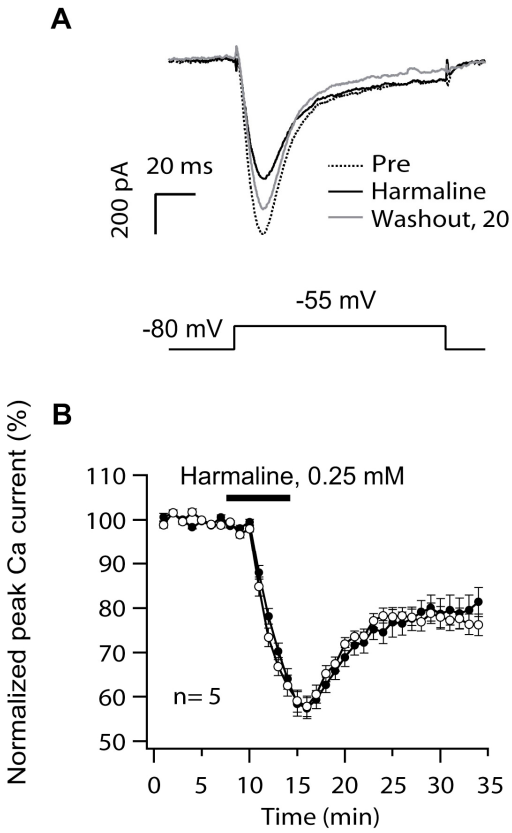

Figure 4. Harmaline, at a concentration of 0.25 mM, attenuates LVA Ca^{2+} currents. These experiments were performed using a recording protocol with no hyperpolarizing prepulse. A) Exemplar current traces recorded from a single olivary neuron. Peak current is plotted for the LVA Ca^{2+} currents evoked by steps to -55 mV during application of 0.25 mM harmaline. B) Population time course records normalized to the baseline period 6-8 min.

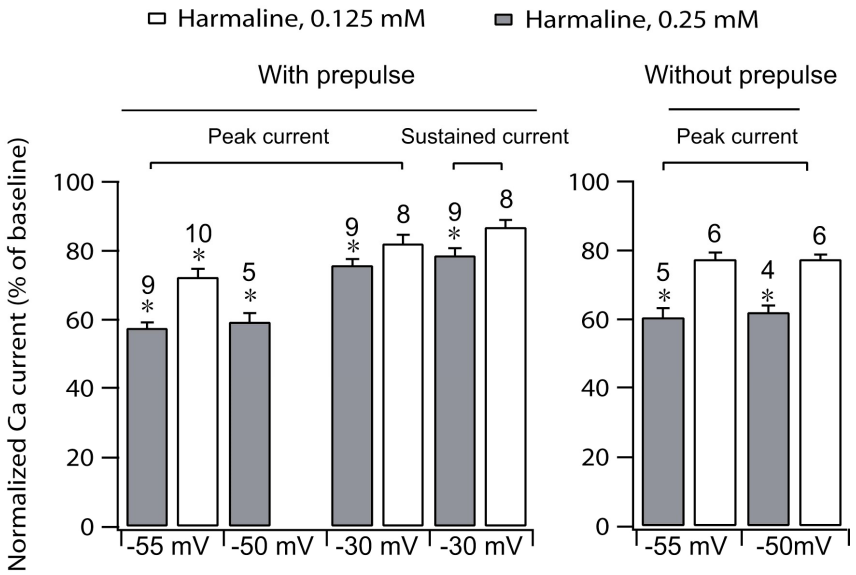

Figure 5. A summary graph showing inhibition of HVA and LVA Ca^{2+} currents by harmaline using various depolarization protocols. The numbers above each bar are the N for that group. Asterisks indicate significant difference from pre-harmaline treatment (*$P<0.05$).

Figure 6

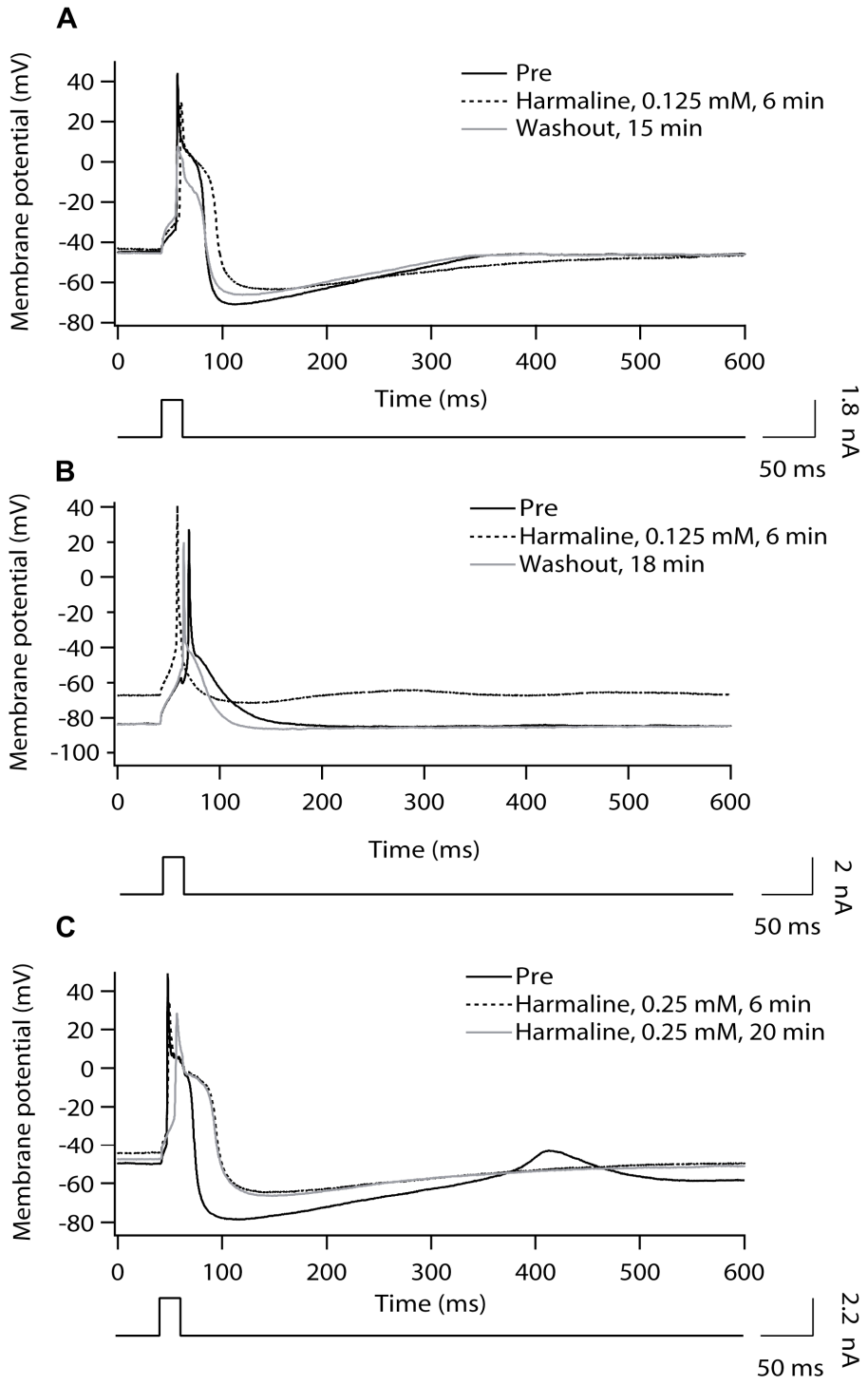

Figure 6. Harmaline broadens Ca^{2+} spikes, attenuates AHPs and sometimes produced hyperpolarization. Current traces from three exemplar cells are shown (from a population of 21). A) A cell with a resting potential of ~ - 44 mV showed no hyperpolarization upon harmaline application, but exhibited broadening of a high-threshold Ca^{2+} spike and AHP attenuation. B) A cell with a resting potential of ~ -66 mV showed significant hyperpolarization upon harmaline application and broadening of the low-threshold Ca^{2+} spike. C) A cell with a resting potential of ~ -50 mV showed no hyperpolarization upon harmaline application and, in fact, displayed a modest depolarization. Broadening of the high-threshold Ca^{2+} spike and attenuation of the AHP are evident.

Our results address and extend these observations in some useful ways. First, we find that both LVA and HVA Ca^{2+} conductances are affected by harmaline. This is consistent with our observation that both low and high-threshold spikes show broadening/AHP attenuation. Second, we find that harmaline produces attenuation, not enhancement of LVA and HVA Ca^{2+} currents and this attenuation is seen in conditions where LVA channel inactivation is largely removed by a hyperpolarizing prepulse. One caveat in interpreting our results is that our recordings were made in newborn tissue which may have different properties than that seen in the adult inferior olive. Our results are in general agreement with those of Splettstoesser et al. who studied harmaline effects on Ca^{2+} currents in cultured rat dorsal root ganglion neurons (22). They reported attenuation of both LVA and HVA Ca^{2+} currents by 0.1 mM harmaline, although in their recordings, the effect on HVA current was somewhat larger than that on LVA current, whereas our recordings from olivary neurons showed the opposite sensitivity. It is also worthwhile noting that higher doses of harmaline (to 0.5 mM) also produced small attenuations of voltages-sensitive Na^+ and K^+ conductances in dorsal root ganglion neurons (22).

Neurons in the inferior olive show strong subthreshold oscillations (18, 35) and these become widespread around postnatal day 16 in rats (32). Neurons in the inferior olive are also electrotonically coupled (36) by gap junctions (37) that typically require the protein connexin 36 (38). It was hypothesized that gap junctional coupling was required to synchronize the activity of a population of olivary neurons and thereby generate the tremor and ataxia produced by harmaline (39, 40). However, while connexin 36 null mice showed asynchronous oscillatory activity in simultaneously recorded neuron pairs, they still showed robust tremors and ataxia in response to harmaline (38). This result suggests that electrotonic coupling is not necessary for the tremorgenic effects of harmaline.

Several lines of evidence indicate that the inferior olive is the primary action site of harmaline for tremorgenesis and ataxia (8, 9, 17, 41). However, the actions of harmaline that produce activation of olivary neurons remain incompletely described and are likely to be complex given the wide range of harmaline's molecular targets. Here we show that harmaline attenuates LVA and HVA Ca^{2+} currents in olivary neurons and produces spike broadening and AHP attenuation. We suggest that these phenomena are related through a reduction in the activation of Ca-sensitive K^+ channels. Interestingly, in *in vivo* recordings in Purkingje cells, apamin increases rhythmicity in complex spikes, whereas charybdotoxin causes decreased rhythmic complex spikes (42). Harmaline has similar effect to that of apamin (43), which suggests an apamin-sensitive K^+ channel is essential for the underling mechanism. Further work conducted in slices of the inferior olive indicated that apamin- but not charybdotoxin-sensitive Ca^{2+} activated K^+ currents play a major role in the afterhyperpolarization (44). Nevertheless, our hypothesis awaits testing in future work.

The harmaline effect on HVA and LVA causes increased excitability of olivary neurons, causing excessive glutamate release at climbing fiber-PC synapses, which triggers Purkinje cell apoptosis (45). Presumably, harmaline effects to both HVA and LVA on Purkinje cells also attenuate Ca^{2+} entry into the cells, which protect the cells from death, since excessive intracellular Ca^{2+} increase also triggers apoptosis (23). In addition, harmaline inhibits monoamine oxidase directly to reduce free radicals and block the oxidative pathway, a key process to trigger glutamate neuronal toxicity (6). The overall harmaline effect is an interplay between its neurotoxic and protective effects that cause tremor as well as ataxia.

CONCLUSIONS

These data suggest that one mode of olivary neuron activation by harmaline involves attenuation of both HVA and LVA Ca^{2+} conductances and consequent attenuation of Ca-sensitive K^+ conductances resulting in spike broadening and attenuation of the afterhyperpolarization, which triggers tremorgenesis. HVA and LVA attenuation also implicates its role, to a lesser extent in ataxia, and neuroprotection of neuronal apoptosis.

ACKNOWLEGEMENTS

We thank Dr. David Linden for generous support and Drs. Jung Hoon Shin, and Yu Shin Kim, for technical help. This work was supported by NIH MH51106 and the Develbiss Fund to David J. Linden, and in part by NSF PIRE program (OISE-0730255) to Werner M. Graf.

REFERENCES

1. May T, Greube A, Strauss S, Heineke D, Lehmann J, Rommelspacher H: Comparison of the in vitro binding characteristics of the beta-carbolines harman and norharman in rat brain and liver and in bovine adrenal medulla. *Naunyn Schmiedebergs Arch Pharmacol* 1994, 349(3):308-317.
2. Rommelspacher H, Nanz C, Borbe HO, Fehske KJ, Muller WE, Wollert U: 1-Methyl-beta-carboline (harmane), a potent endogenous inhibitor of benzodiazepine receptor binding. *Naunyn Schmiedebergs Arch Pharmacol* 1980, 314(1):97-100.
3. McCormick SJ, Tunnicliff G: Inhibitors of synaptosomal gamma-hydroxybutyrate transport. *Pharmacology* 1998, 57(3):124-131.
4. Anderson NJ, Robinson ES, Husbands SM, Delagrange P, Nutt DJ, Hudson AL: Characterization of [(3)H]harmane binding to rat whole brain membranes. *Ann N Y Acad Sci* 2003, 1009:175-179.
5. Glennon RA, Dukat M, Grella B, Hong S, Costantino L, Teitler M, Smith C, Egan C, Davis K, Mattson MV: Binding of beta-carbolines and related agents at serotonin (5-HT(2) and 5-HT(1A)), dopamine (D(2)) and benzodiazepine receptors. *Drug Alcohol Depend* 2000, 60(2):121-132.
6. Maher P, Davis JB: The role of monoamine metabolism in oxidative glutamate toxicity. *J Neurosci* 1996, 16(20):6394-6401.
7. Batini C, Buisseret-Delmas C, Conrath-Verrier M: Harmaline-induced tremor. I. Regional metabolic activity as revealed by [14C]2-deoxyglucose in cat. *Exp Brain Res* 1981, 42(3-4):371-382.
8. Milner TE, Cadoret G, Lessard L, Smith AM: EMG analysis of harmaline-induced tremor in normal and three strains of mutant mice with Purkinje cell degeneration and the role of the inferior olive. *J Neurophysiol* 1995, 73(6):2568-2577.
9. Simantov R, Snyder SH, Oster-Granite ML: Harmaline-induced tremor in the rat: abolition by 3-acetylpyridine destruction of cerebellar climbing fibers. *Brain Res* 1976, 114(1):144-151.
10. Sladek JR, Jr., Bowman JP: The distribution of catecholamines within the inferior olivary complex of the cat and rhesus monkey. *J Comp Neurol* 1975, 163(2):203-213.
11. Deuschl G, Elble RJ: The pathophysiology of essential tremor. *Neurology* 2000, 54(11 Suppl 4):S14-20.
12. Louis ED, Zheng W, Jurewicz EC, Watner D, Chen J, Factor-Litvak P, Parides M: Elevation of blood beta-carboline alkaloids in essential tremor. *Neurology* 2002, 59(12):1940-1944.
13. Martin FC, Handforth A: Carbenoxolone and mefloquine suppress tremor in the harmaline mouse model of essential tremor. *Mov Disord* 2006, 21(10):1641-1649.
14. Miwa H: Rodent models of tremor. *Cerebellum* 2007, 6(1):66-72.
15. Jones N, Le Marec N, Stelz T, Caston J: Effect of administration of 3-acetylpyridine followed by niacinamide injection on survival, extent of the inferior olivary complex lesion, and response to harmaline in the young rat. *Brain Res* 1994, 656(2):257-262.
16. Llinás R, Volkind RA: The olivo-cerebellar system: functional properties as revealed by harmaline-induced tremor. *Exp Brain Res* 1973, 18(1):69-87.
17. Park YG, Park HY, Lee CJ, Choi S, Jo S, Choi H, Kim YH, Shin HS, Llinás RR, Kim D: Ca(V)3.1 is a tremor rhythm pacemaker in the inferior olive. *Proc Natl Acad Sci U S A* 2010, 107(23):10731-10736.
18. Llinás R, Yarom Y: Oscillatory properties of guinea-pig inferior olivary neurones and their pharmacological modulation: an in vitro study. *J Physiol* 1986, 376:163-182.
19. Handforth A, Homanics GE, Covey DF, Krishnan K, Lee JY, Sakimura K, Martin FC, Quesada A: T-type calcium channel antagonists suppress tremor in two mouse models of essential tremor. *Neuropharmacology* 2010, 59(6):380-387.
20. Ertel EA, Campbell KP, Harpold MM, Hofmann F, Mori Y, Perez-Reyes E, Schwartz A, Snutch TP, Tanabe T, Birnbaumer L *et al*: Nomenclature of voltage-gated calcium channels. *Neuron* 2000, 25(3):533-535.
21. Choi S, Yu E, Kim D, Urbano FJ, Makarenko V, Shin HS, Llinás RR: Subthreshold membrane potential oscillations in inferior olive neurons are dynamically regulated by P/Q- and T-type calcium channels: a study in mutant mice. *J Physiol* 2010, 588(Pt 16):3031-3043.
22. Splettstoesser F, Bonnet U, Wiemann M, Bingmann D, Busselberg D: Modulation of voltage-gated channel currents by harmaline and harmane. *Br J Pharmacol* 2005, 144(1):52-58.
23. Han OJ, Joe KH, Kim SW, Lee HS, Kwon NS, Baek KJ, Yun HY: Involvement of p38 mitogen-activated protein kinase and apoptosis signal-regulating kinase-1 in nitric oxide-induced cell death in PC12 cells. *Neurochem Res* 2001, 26(5):525-532.
24. Ye JH, Zhang J, Xiao C, Kong JQ: Patch-clamp studies in the CNS illustrate a simple new method for obtaining viable neurons in rat brain slices: glycerol replacement of NaCl protects CNS neurons. *J Neurosci Methods* 2006, 158(2):251-259.
25. Paxinos G, Watson C: *The Rat Brain in Stereotaxic Coordinates, Academic Press. 4th edition* 4rd edition. San Diego: Academic Press. ; 1998.
26. Talbot MJ, Sayer RJ: Intracellular QX-314 inhibits calcium currents in hippocampal CA1 pyramidal neurons. *J Neurophysiol* 1996, 76(3):2120-2124.

27. Hu GY, Biro Z, Hill RH, Grillner S: Intracellular QX-314 causes depression of membrane potential oscillations in lamprey spinal neurons during fictive locomotion. *J Neurophysiol* 2002, 87(6):2676-2683.
28. Eckert R, Chad JE, Kalman D: Enzymatic regulation of calcium current in dialyzed and intact molluscan neurons. *J Physiol (Paris)* 1986, 81(4):318-324.
29. Horn R, Korn SJ: Prevention of rundown in electrophysiological recording. *Methods Enzymol* 1992, 207:149-155.
30. Mouginot D, Bossu JL, Gähwiler BH: Low-threshold Ca^{2+} currents in dendritic recordings from Purkinje cells in rat cerebellar slice cultures. *J Neurosci* 1997, 17(1):160-170.
31. Regan LJ: Voltage-dependent calcium currents in Purkinje cells from rat cerebellar vermis. *J Neurosci* 1991, 11(7):2259-2269.
32. Bleasel AF, Pettigrew AG: Development and properties of spontaneous oscillations of the membrane potential in inferior olivary neurons in the rat. *Brain Res Dev Brain Res* 1992, 65(1):43-50.
33. Llinás R, Yarom Y: Properties and distribution of ionic conductances generating electroresponsiveness of mammalian inferior olivary neurones in vitro. *J Physiol* 1981, 315:569-584.
34. Llinás R, Yarom Y: Electrophysiology of mammalian inferior olivary neurones in vitro. Different types of voltage-dependent ionic conductances. *J Physiol* 1981, 315:549-567.
35. Benardo LS, Foster RE: Oscillatory behavior in inferior olive neurons: mechanism, modulation, cell aggregates. *Brain Res Bull* 1986, 17(6):773-784.
36. Devor A, Yarom Y: Electrotonic coupling in the inferior olivary nucleus revealed by simultaneous double patch recordings. *J Neurophysiol* 2002, 87(6):3048-3058.
37. Bourrat F, Sotelo C: Postnatal development of the inferior olivary complex in the rat. I. An electron microscopic study of the medial accessory olive. *Brain Res* 1983, 284(2-3):291-310.
38. Long MA, Deans MR, Paul DL, Connors BW: Rhythmicity without synchrony in the electrically uncoupled inferior olive. *J Neurosci* 2002, 22(24):10898-10905.
39. Chorev E, Manor Y, Yarom Y: Density is destiny--on [corrected] the relation between quantity of T-type Ca^{2+} channels and neuronal electrical behavior. *CNS Neurol Disord Drug Targets* 2006, 5(6):655-662.
40. Yarom Y: Rhythmogenesis in a hybrid system--interconnecting an olivary neuron to an analog network of coupled oscillators. *Neuroscience* 1991, 44(2):263-275.
41. De Montigny C, Lamarre Y: Effects produced by local applications of harmaline in the inferior olive. *Can J Physiol Pharmacol* 1975, 53(5):845-849.
42. Lang EJ, Sugihara I, Llinás R: Differential roles of apamin- and charybdotoxin-sensitive K+ conductances in the generation of inferior olive rhythmicity in vivo. *J Neurosci* 1997, 17(8):2825-2838.
43. Lorden JF, Stratton SE, Mays LE, Oltmans GA: Purkinje cell activity in rats following chronic treatment with harmaline. *Neuroscience* 1988, 27(2):465-472.
44. Bal T, McCormick DA: Synchronized oscillations in the inferior olive are controlled by the hyperpolarization-activated cation current I(h). *J Neurophysiol* 1997, 77(6):3145-3156.
45. O'Hearn E, Molliver ME: Degeneration of Purkinje cells in parasagittal zones of the cerebellar vermis after treatment with ibogaine or harmaline. *Neuroscience* 1993, 55(2):303-310.